Analysis and modeling of the dispersion of vaporizing polydispersed sprays in turbulent flows

By J. Réveillon †, M. Massot ‡ AND C. Pera ¶

Direct numerical simulations (DNS) of turbulent two-phase flows have been carried out to study the polydispersion of a vaporizing spray in statistically-stationary grid turbulence. The evolution of various classes of droplet size has been studied, exhibiting different dynamical behavior for droplets of different sizes. The results have been used to evaluate successfully a new Eulerian model, which proves its ability to capture the polydisperse spray dynamics and vaporization.

1. Introduction

In industrial combustion configurations, the fuel is most of the time injected as a dispersed phase of liquid droplets. In gas turbines, diesel engines, industrial furnaces and combustion chambers, the behavior of the gaseous fuel mixture fraction plays a crucial role in determining the combustion characteristics and efficiency of the process. Consequently, the description of the motion of the spray, its vaporization and its coupling with the gaseous turbulent flow field are important for the prediction of two-phase turbulent combustion. Even if the process has to be understood as a whole from injection up to combustion, one of the key issues will be the turbulent mixing and vaporization of the cloud of fuel droplets, a phenomenon strongly influenced by the polydisperse character of the spray. In this paper, we therefore focus our attention on the turbulent dispersion of a vaporizing liquid spray and on its polydispersion.

The purpose of the present study is two-fold: first, we investigate the physics of this phenomenon using a DNS Euler/Lagrange approach in the configuration of statistically-stationary spatially decaying turbulence, with a monodisperse injection. We analyze the DNS results for the dispersed phase from an Eulerian point of view, and demonstrate the strong coupling of the dynamics and vaporization which generates droplets of various sizes. Second, we provide a Eulerian model and description of this phenomenon, extending the recently-introduced Eulerian multi-fluid models which are well suited to the presence of a polydisperse spray. These approaches will then be compared, thus proving the ability of the Eulerian model to capture the physics and the complementarity of Lagrangian and Eulerian tools for the description of two-phase flows.

Two types of models may be actually considered for the description of the polydisperse liquid phase. The first one is of Lagrangian and particular type as described originally by Dukowicz (1980), O'Rourke (1981). The distribution of droplets is approximated using a finite number of computational parcels; each parcel represent a number of droplets of identical size, velocity and temperature. This kind of method is currently used in

† CNRS-UMR 6614 - CORIA - University of Rouen, INSA - Avenue de l'Université, 76801 St Etienne du Rouvray cdx, FRANCE, reveillon@coria.fr, corresponding author
‡ CNRS-UMR5585 - MAPLY, Université Claude Bernard, Lyon 1, 69622 Villeurbanne cdx, FRANCE, massot@maply.univ-lyon1.fr
¶ CNRS-UMR 6614 - CORIA, pera@coria.fr

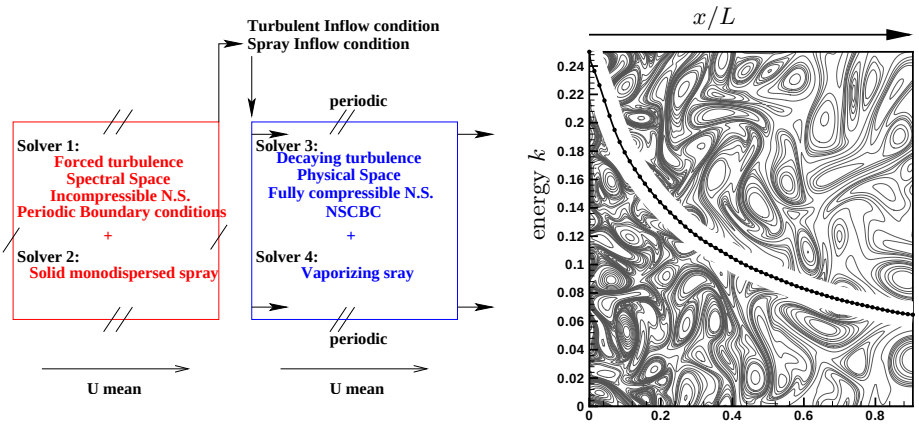

Light	τ_p/τ_v	τ_p/τ_t	evaporation	Heavy	τ_p/τ_v	τ_p/τ_t	evaporation
T0V0	195	0.06	$s = cte$	**T2V0**	3.5	3.3	$s = cte$
T0V1	195	0.06	$s/s_0 = 1 - t/\tau_v$	**T2V1**	3.5	3.3	$s/s_0 = 1 - t/\tau_v$

FIGURE 1. Left: sketch of the coupling between the four solvers, right: vorticity isocontours of the decaying turbulence, bottom: data concerning the injected droplets for each simulation.

many codes and is especially suited for DNS calculations since it does not introduce any numerical diffusion, the particle trajectories in the phase space being exactly resolved. It is then particularly accurate as long as the sampling of the phase space is rapid enough, a constraint that becomes expensive for unsteady flows.

In the context of RANS and LES numerical simulations, where some scales are not resolved but modeled, the perspective of a Eulerian model for polydisperse sprays becomes very attractive. Indeed, it is interesting to study the Eulerian form of the spray equations and to deduce the structure of physical phenomena such as waves, diffusion, etc. On another hand, modeling of coalescence and break-up phenomena, as well as the coupling with the combustion process, is more straightforward using an Eulerian formulation. Besides, a coherent way of treating the two phases yields a better ability for parallel computations and optimization.

The existing Eulerian models belong to the broad class of moment methods and can be subdivided into two general branches. On the one side, the population-balance methods usually consider very small particles without inertia. They are concerned with a precise description of the size distribution which evolves due to vaporization, aggregation or breakage – see e.g. Wright et al. (2001), Marchisio, Vigil & Fox (2002) – and usually rely on the method of quadrature of size moments. On the other side, the classical two-fluid models have been the subject of many publications, either in the mathematics community by Sainsaulieu (1991), Domelevo & Sainsaulieu (1997) or in the engineering one (see Kaufmann et al. (2002) and references therein). Their validity extends up to churning flows where the liquid phase is not dispersed any more such as near the injector (Vallet et al., 2001) or for interface phenomena such as in Chanteperdrix et al. (2002).

However, actual Eulerian models present two major drawbacks: the inability to capture the polydispersion in size of the spray (only through a couple of moments such as in Vallet

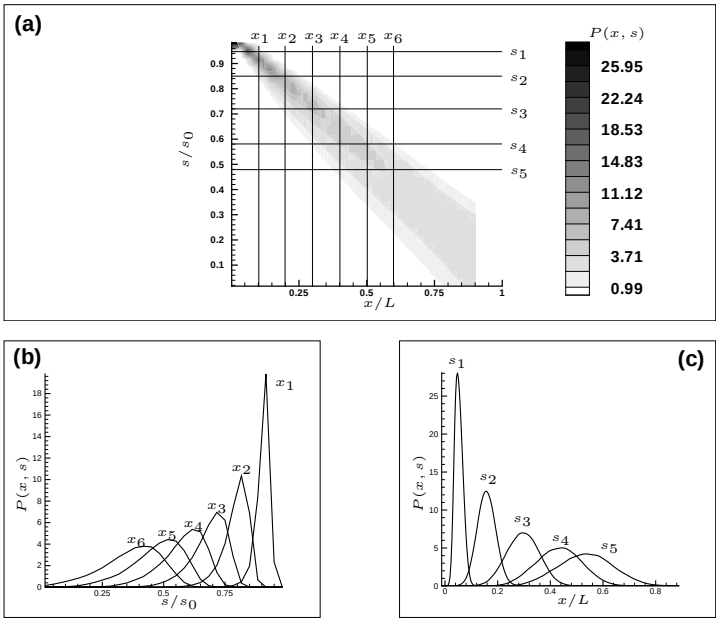

FIGURE 2. Isocontours (top) and profiles (bottom left and right) of the pdf $P(s,x)$. The profiles are made along both x (bottom right) and s (bottom left) directions for several different positions shown on the top figure. $x_1/L = 0.092$, $x_2/L = 0.198$, $x_3/L = 0.304$, $x_4/L = 0.41$, $x_5/L = 0.516$, $x_6/L = 0.622$, and $s_1/s_0 = 0.95$, $s_2/s_0 = 0.85$, $s_3/s_0 = 0.72$, $s_4/s_0 = 0.58$, $s_5/s_0 = 0.48$

et al., 2001) and the lack of direct link with the kinetic level of description for sprays. Thus, in the context of laminar flows, Laurent and Massot (2001) have introduced a multi-fluid approach, rigorously derived from the kinetic level of description, which has the capability to include coalescence and break-up as shown in Laurent et al. (2001) and to describe the vaporization, dynamics and heating of droplets of various sizes as studied in Laurent et al. (2002). In order to extend the work done in these papers to turbulent flows and derive a kinetic model "in the mean" where an ensemble averaging is performed on some scales, we make use of the results introduced by Reeks (1991) and proved by Clouet and Domelevo (1997), and connect with the work on Eulerian analysis of the turbulent dispersion of particles initiated by Taylor (1921) and Batchelor (1949). An Eulerian system of semi-fluid equations is obtained by preserving the size phase space but considering some velocity-moment closure. We then show the ability of such an approach to capture the physics of the turbulent dispersion of a vaporizing spray by comparing with success the results from the Eulerian model to DNS statistics. We show in particular that the use of surface-conditioned moments is really well-suited to characterize the phenomenon and to obtain a precise Eulerian description.

The paper is organized as follows: in a second section, the physical configuration and numerical methods are presented. We then focus on the analysis of the DNS results where we emphasize a surface-conditioned Eulerian analysis of the polydisperse spray. We then conduct, in a fourth section, the derivation of the Eulerian model and present the numerical method used in the particular configuration under consideration. The DNS results and the simulations obtained from the Eulerian solver are then compared in the last section.

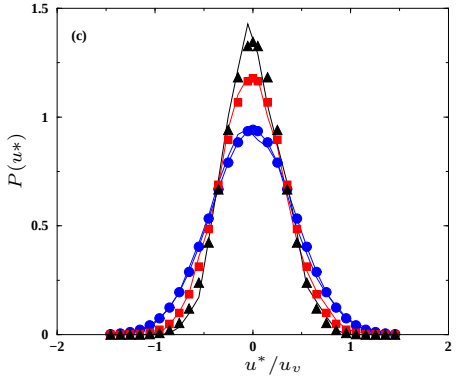

FIGURE 3. Profiles of $P(u)$, lines: DNS extracted, symbols: corresponding Gaussian reconstruction (circles: x_1, squares: x_3 and triangles: x_6).

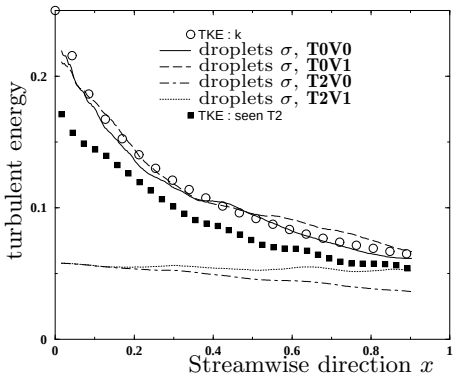

FIGURE 4. Comparison of the spatial evolution of the droplets energy σ with the gas turbulent kinetic energy k.

2. Geometry and numerical considerations

In this paper, a geometry with one inhomogeneous direction has been considered: 2D spatially-decaying turbulence (SDT) with statistically-stationary properties. It simulates grid turbulence with a high kinetic energy at the inlet that decays in the streamwise direction. A monodisperse spray is injected through the inlet boundary and follows the main flow while being locally dispersed by the turbulent fluctuations. It is particularly interesting to notice that the coupling of vaporization and turbulent mixing generates a polydisperse spray, even if the liquid phase is injected monodisperse. This configuration is also a good candidate since the number of dimensions of the phase space remains reasonable.

To ensure statistically-coherent behavior of the injected droplets with local turbulence, four solvers (figure 1) are running simultaneously. An independent spectral code is solving the incompressible Navier-Stokes (NS) equations, coupled with a one-way Lagrangian solver for the computation of the dispersion of solid particles. These two solvers are used to generate accurate turbulent boundary conditions for a physical-space DNS solver (sixth order in space and third order in time) running together with another one-way Lagrangian solver. The fully-compressible NS equations are then solved with periodic boundary conditions along the spanwise direction, and NS characteristic boundary conditions (Poinsot and Lele, 1992) for the inlet and the outlet along the streamwise direction.

Forced turbulence, such as in Overholt and Pope, 1998, is simulated in the spectral space so that the prescribed main properties of the turbulence (kinetic energy, dissipation, integral scale) are statistically stationary in time. The dispersion of particles in the phase space was checked to be in dynamical equilibrium before the coupling with the physical space solvers took place.

This coupling is done through the inlet boundary of the physical space solver where the turbulent fluctuations as well as the incoming particles are inserted. Because of the presence of the spectral solver, the vortices are really able to rotate at the boundary and therefore, local negative velocities may be considered. The technical details of the injection procedure may be found in Vervisch-Guichard et al. (2001). Once injected in the physical space DNS, the previously-solid particles are considered as droplets of liquid

and they vaporize, following a *d-square* law, and undergo the effects of drag forces. Again, a one-way interaction with the turbulent flow is used to describe the dispersion of the droplets. It allows us to keep identical turbulence parameters while the spray properties are modified.

Before presenting the various test cases and results of this work, normalization parameters should be introduced. They are based on the properties of the flow and the spray. The droplet geometry is expressed in term of a surface and it is normalized by their unique (monodisperse) injection value s_0. The motion of the droplets in the gaseous flow and their evaporation rate lead to the characteristic times τ_p and τ_v; τ_p is the velocity response time (or kinetic time) of the droplets, quantifying their ability to follow or not the fluctuations of the flow, and $\tau_v = -s_0/\mathcal{R}$ is the vaporization time based on the initial size. They have to be compared with τ_t, the turbulent eddy turnover time. It leads to the following normalized *d-square* law: $s/s_0 = 1 - t/\tau_v$. The other parameters are the career phase mean velocity $\overline{\mathbf{U}}$ and consequently, the characteristic distance $L = \overline{\mathbf{U}} * \tau_v$ covered by a droplet before its total vaporization.

3. Spray turbulent dispersion

3.1. *Statistical considerations*

The study of the dispersion of droplets in spatially-decaying turbulence implies to define some new parameters. An individual tracking has been introduced for every droplet in the flow whose Lagrangian time, position, velocity and surface are (t_l, $\mathbf{x_d}$, $\mathbf{V}_d$, $s_d(t_l)$). As soon as a droplet is injected and begins to evaporate, it is associated to a 'reference particle' whose initial properties (t_l, $\mathbf{x_r}$, $\overline{\mathbf{U}}$, $s_r = s_d$) are the same. The reference particle travels at the mean streamwise velocity, whereas its corresponding droplet is affected by turbulent fluctuations. By statistically studying the difference of position and velocity between the real droplet and its 'reference', we may characterize the turbulent dispersion. The dispersion statistics are then deduced from the following parameters: $\mathbf{x}^* = \mathbf{x_d} - \mathbf{x_r}$, $\mathbf{v}^* = \mathbf{V_d} - \overline{\mathbf{U}}$ and $\xi = s_d - s_0(1 - x_d/L)$. ξ is the relative surface between the tracked droplet and a droplet that would be at the same position if unaffected by turbulence.

Statistics are considered in time and along the spanwise direction. Therefore the mean value of any Eulerian variable $A(x, y, t)$ is defined by the following relation

$$\overline{A}(x) = \frac{1}{T} \int \left(\frac{1}{L_y} \int \int A(x, y, t) dy \right) dt. \tag{3.1}$$

3.2. *Spray polydispersion*

Figure 2-(a) shows an example of the evolution of the coupled PDF: $P(x, s)$ of the droplets streamwise position x and their surface s. It allows us to observe the **joint** effects of the evaporation and of the turbulence on the injected spray. Several positions of analysis along both x and s directions have been plotted. These positions, labeled respectively x_i ($i = 1$ to 6) and s_j ($j = 1$ to 5), have been extensively used in this work. The profiles of $P(x, s)$ along the x direction for the fixed surfaces s_j show (figure 2(c)) a symmetrical Gaussian dispersion around a reference position $x_j^r/L = (1 - s_j/s_0)$ corresponding to the position of a droplet with the same s_j surface but which was not affected by turbulence. Similarly, a spreading of the droplets surface may be observed (figure 2(b)) for a given x_i streamwise position. But, in contrast with the previous profiles, the dispersion is not symmetric around the reference surface $s_i^r/s_0 = (1 - x_i/L)$, corresponding to the surface of a vaporizing droplet moving with the reference velocity $\overline{\mathbf{U}}$.

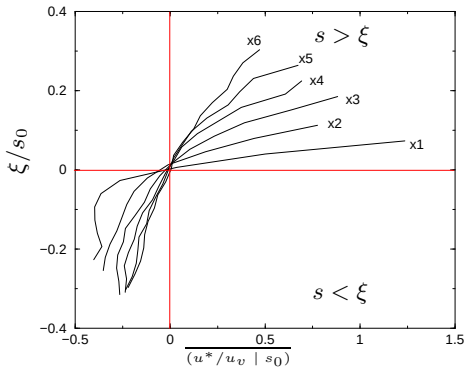

FIGURE 5. Mean droplet velocity conditioned by the droplet surface (**T0V1**, Eulerian positions: $x_i,\ i = 1, 6$).

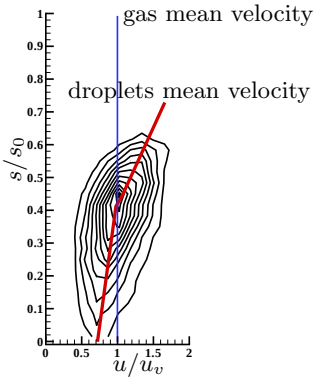

FIGURE 6. Comparisons of the spray velocity dispersion function $P(u, s)$ (black lines) with an assumed Gaussian shape dispersion function (dotted lines), case **T0V1**, Eulerian position: x_6.

It is possible to examine the PDF: $P(u^*)$ corresponding to the droplet velocity fluctuations with respect to the gas mean flow. Indeed, as will be shown later, a distinction has to be made between the gas-phase mean velocity and the particle mean velocity. The u^* statistics have been evaluated for all droplets without distinction of class, and a Gaussian shaped dispersion may be observed along the streamwise direction. Figure 3 shows that $P(u^*)$ develops a general Gaussian shape centered on $u^* = 0$. Three profiles of $P(u^*)$ extracted from the DNS are plotted in figure 3(a) along with the corresponding PDF deduced from the first two moments $(\overline{u}^*, \sigma)$ of the velocity dispersion. A Gaussian shape function (4.3) has been used, and σ has been determined from the values of $P(u^*)$ extracted from the DNS. The assumed Gaussian shape and the DNS data are similar. This confirms a Gaussian behavior of dispersion for the droplets considered as a whole, without reference to their size. Moreover, the fact that the Gaussian curves are centered on $u^* = 0$ shows that the mean droplet velocity is equal to the mean flow velocity (as long as the droplets are not considered by classes).

The droplet energy σ has been determined for every streamwise position and is compared to the decaying kinetic energy k of the gas flow in figure 4. For each droplet family, vaporizing and non-vaporizing cases have been plotted. As expected, it is possible to observe a mass-dependent behavior of the droplets. The light droplets (**T0Vx**, x= $0, 1$), with a small Stokes number ($S_t = 0.06$), closely follows the turbulent fluctuations of the gas. As soon as the droplets' mass (and therefore Stokes number) increases (**T2Vx**), the inertia of the droplets is increasingly significant and they no longer exactly capture the fluctuations of the carrier phase. Thus, for a given spray, three energy levels can be differentiated according to the characteristic kinetic time of the droplets: k the real level of the gas kinetic energy, κ_p the level seen by the droplets and σ the level reached by the droplets. For light droplets with small τ_p, these levels coincide. As soon as τ_p increases, the three levels are differentiated with a fixed hierarchy: $k > \kappa_p > \sigma$.

3.3. *Surface-conditioned dispersion*

The spray is initially monodisperse but it undergoes the effects of both droplet vaporization and turbulent mixing. These two phenomena lead to a polydisperse spray in both x

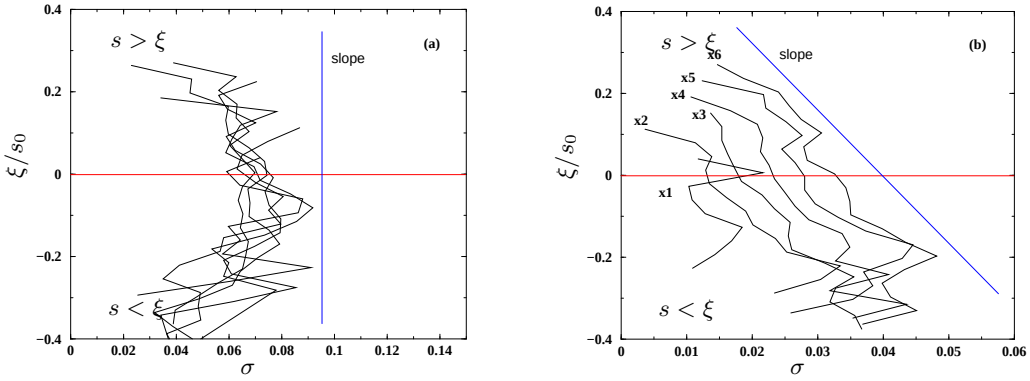

FIGURE 7. Droplet velocity dispersion parameter σ as a function of the droplet relative surface ξ. Left: **T0V1** case, the profiles are similar, right: **T1V1** case a significant effect of the droplet volume may be observed on the dispersion.

and s directions of the phase space. In the previous section it was shown that the spray position dispersion for a fixed droplet surface follows a Gaussian behavior. Now, it seems interesting to focus on the velocity behavior of the droplets considered class by class.

First, from an analytical point of view, it is possible to affirm that the mean velocities of the droplets depend on their surface for a given Eulerian position x. At any x position, by using the reference parameters ξ and u^*, we know that the droplets such as $\xi = 0$ and $u^* = 0$ have the same mean properties as the reference droplets which are supposed unaffected by the turbulence. If $\xi > 0$, then the droplet surface is larger than the reference one. Thus, these droplets traveled more quickly than the average flow. In the same way, the droplets such as $\xi < 0$ went more slowly. This is confirmed by figure 5 where the mean droplet velocity conditioned by droplet surface $\overline{(u^* \mid \xi)}$ has been plotted. The analysis has been done for several Eulerian positions previously defined (figure 2). Close to the injection (x_1), the surface range dispersion is limited but, because of the high turbulent energy of the flow, velocity levels of the droplets are the highest. As the droplets move away in the flow, their surface range increases but their mean velocity range decreases because of the weaker turbulent mixing.

The conditioned mean velocity being known, it is now particularly interesting to focus on the velocity dispersion of the droplets around this mean. Figure 6 shows, for a given streamwise position, the PDF $P(u, s)$ representing the velocity dispersion as a function of the droplet surface. Gaussian reconstructions around this mean value have been carried out. The deduced isocontours are shown figure 6 (dotted contours) and are very close to the dispersion levels extracted from the DNS (plain contours). It appears that even by considering the dispersion as a function of the droplets surface, it follows a Gaussian law. But this is true only around the mean velocity of the particles and not around the local mean velocity of the gas flow, the two of them being different. Moreover, an integration of the dispersion along the s direction gives a global Gaussian dispersion around the mean flow velocity (figure 3). But the corresponding energy σ is a global property for the whole spray and it does not allow a description of the dynamic of every class of droplets. This dynamic depends strongly on the mass of the droplets; thus, to have an accurate description of their dispersion, a surface dependence should be introduced in any model developed to describe the dispersion of evaporating or polydisperse droplets.

Examples of the surface-conditioned energy $\sigma(\xi)$ are shown figure 7 for both **T0V1**

and **T2V1** cases. The statistics have been extracted for the reference Eulerian positions and correspond to the agitation energy of the droplets around their mean velocity. For the whole Eulerian positions, the light droplets have a similar $\sigma(\xi)$ whatever the droplet surface is. In fact, even the 'heaviest' ($\xi > 0$) of the light droplets (**T0V1**) are small and follow the turbulent fluctuations of the carrier phase without noticeable damping due to their inertia. Therefore, $\sigma(\xi)$ is almost constant for every value of the surface. On another hand, the vaporizing heavy droplets case (**T2V1**) leads to another conclusion. Indeed, because of their large Stokes number, the droplets prove to have an inertial behavior, going through turbulent structures without fully undergoing every one of them. Two main conclusions can be drawn from the figure 7-(b). First of all, for every increasing analysis Eulerian position (x_1, x_2, ...) the general energy level $\sigma(\xi)$ increases as well, because the droplets' loss of mass implies a decrease of the effects of their inertia. In the same way, for a given analysis position, the dependence of $\sigma(\xi)$ on the surface of the droplets (ξ) is significant and has a quasi-linear behavior.

4. Multi-fluid modeling

The fact that the turbulent dispersion of a vaporizing spray is a surface-conditioned phenomenon is very coherent with the work done on the Eulerian multi-fluid modeling of polydisperse sprays conducted by Laurent and Massot (2001). The purpose of this section is to present the derivation of such an approach in the turbulent case and the associated numerical methods.

4.1. *Derivation of the model*

The spray is described at the kinetic level by a distribution function $f(t, x, s, \boldsymbol{V}_d)$ which satisfies a transport equation introduced by Williams (1958):

$$\frac{\partial f}{\partial t} + \boldsymbol{V}_d \cdot \nabla_x f + \frac{\partial \mathcal{R}\, f}{\partial s} + \nabla_{\boldsymbol{V}_d}(\mathcal{F}\, f) = 0, \tag{4.1}$$

where $\mathcal{F}$ is the Stokes-drag acceleration. The vaporization rate $\mathcal{R}$ is assumed to be independent of $\boldsymbol{U}$, thus neglecting the convective correction term (see Laurent and Massot (2001) for detailed modeling assumptions).

For turbulent flows, the gas velocity seen by the particles can be decomposed into $\boldsymbol{U} = \overline{\boldsymbol{U}} + \boldsymbol{U}'$, where $\overline{\boldsymbol{U}}$ is its average value and $\boldsymbol{U}'$ is a fluctuation which is assumed to be a Gaussian Wiener process characterized by a Lagrangian correlation time along the trajectories τ_d as well as a turbulent kinetic energy κ_p. It is at this level that we can choose the scales which will be resolved. In this paper, for the first investigation of the Eulerian multi-fluid model, we will consider that the fluctuation describes the whole of the gas turbulence and the average value will be taken as the mean gas velocity. The LES point of view will be investigated in a subsequent study.

Once the scales have been chosen we need to derive a kinetic equation "in the mean" where the effects of the gas turbulence appear only through its characteristic quantities τ_d and κ_p. We use the framework introduced by Reeks (1991) and justified rigorously by Clouet and Domelevo (1997). We obtain an averaged equation for $\bar{f}$, which is the statistical expectation of f; it reads

$$\frac{\partial \bar{f}}{\partial t} + \boldsymbol{V}_d \cdot \nabla_x \bar{f} + \frac{\partial \mathcal{R}\, \bar{f}}{\partial s} + \nabla_{\boldsymbol{V}_d}(\bar{\mathcal{F}}\, \bar{f}) - \nabla_{\boldsymbol{V}_d} \cdot \left(D_x \nabla_x \bar{f} + D_{\boldsymbol{V}_d} \nabla_{\boldsymbol{V}_d} \bar{f} \right) = 0, \tag{4.2}$$

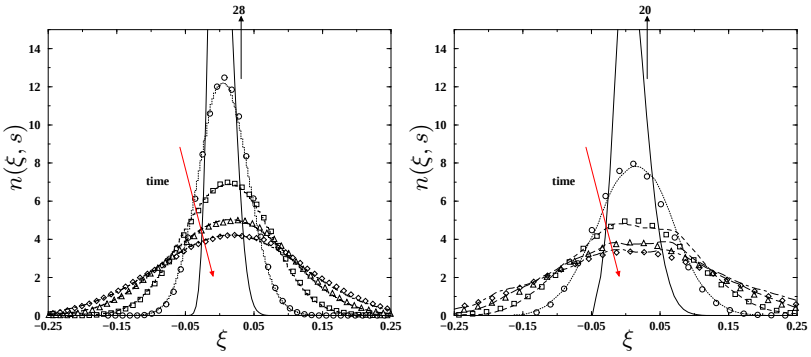

FIGURE 8. Droplet number density in a frame moving with the mean flow for various droplet sizes (or Lagrangian times). Symbols: DNS statistics (circles: s_2, squares: s_3, trianglesd: s_4, diamonds: s_5). Lines (**left**): Eulerian simulations of system (4.4-4.6), **T2V1** case and lines (**right**): Eulerian simulations of the diffusion equation (4.7), **T0V1** case.

where the averaged drag force is

$$\bar{\mathcal{F}} = \frac{1}{\tau_p\, s}(\overline{\boldsymbol{U}} - \boldsymbol{V}_d).$$

The random fluctuations in the gas velocity then generate, on average, a diffusion process in the phase space. This approach requires the use of a simple vaporization model, which decouples the vaporization process from the velocity fluctuations; in a more general case, some additional terms should be added in (4.2). An exact expression of the diffusion coefficients can be obtained as functions of τ_d and κ_p along the lines given in Clouet and Domelevo (1997), Reeks (1991). These coefficients appear in the averaging process where one has to evaluate the statistical expectation of $\boldsymbol{E}(f\boldsymbol{U}')$. This expectation can be proved, under the assumptions made on the alea $\boldsymbol{U}'$, to be a combination of two terms $D_x\,\nabla_x \bar{f} + D_{\boldsymbol{V}_d}\,\nabla_{\boldsymbol{V}_d}\bar{f}$ where the coefficients are deduced from a characteristics analysis.

Once the kinetic equation "in the mean" is derived, we can generalize the framework of the Eulerian multi-fluid model to the present case. As in Laurent and Massot (2001), we make an assumption on $\bar{f}$ which appears as a closure at the kinetic level. We assume that, for a given size, there is only one characteristic velocity, with a Gaussian dispersion around it:

$$\bar{f}(t, x, s, \boldsymbol{V}_d) = n(t, x, s)\,\varphi_{\sigma(t,x,s)}(\boldsymbol{V}_d - \bar{\boldsymbol{V}}_d(t, x, s)),$$

where φ_σ is a Gaussian of dispersion σ in the d-dimensional space:

$$\varphi_\sigma(v) = \frac{1}{\left(\frac{4}{d}\pi\sigma\right)^{d/2}} \exp\left(-\frac{v^2}{\frac{4}{d}\,\sigma}\right). \tag{4.3}$$

We will then obtain the semi-fluid equations on the three moments n, $\bar{\boldsymbol{V}}_d$ and σ, which can be interpreted as an internal energy of a monoatomic gas. It is worth noting that this is a very natural introduction of the "quasi-Brownian" motion in Kaufmann et al. (2002).

We introduce the non-dimensional quantities $\overline{V} = (\overline{\mathbf{V}}_d - \overline{\mathbf{U}})/\overline{\mathbf{U}}$ and $\bar{\sigma} = \sigma/\overline{\mathbf{U}}^2$. From the equation (4.2), we obtain a non-dimensional Eulerian semi-fluid model:

$$\frac{\partial n}{\partial \tau} + \nabla_\xi \cdot (n\overline{V}) - \frac{\partial\, n}{\partial \bar{s}} = 0 \tag{4.4}$$

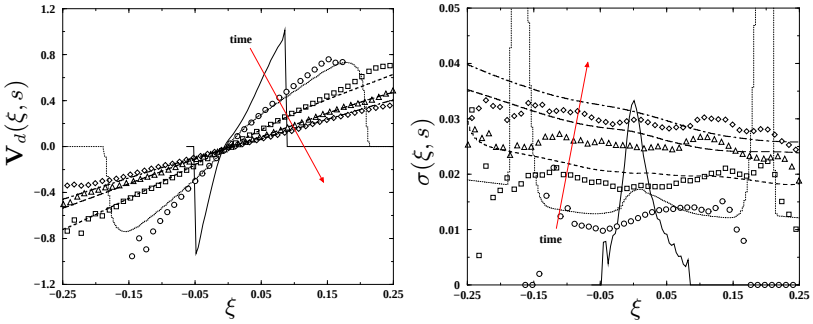

FIGURE 9. Evolution of droplets mean velocity **left** and droplets internal energy **right** in the frame moving with the mean for various droplet sizes in the **T2V1** case. Symbols: DNS statistics (circles: s_2, squares: s_3, triangles: s_4, losanges: s_5). Lines: Eulerian simulations of system (4.4-4.6).

$$\frac{\partial n\,\overline{V}}{\partial \tau} + \nabla_\xi \cdot \left(n\,\overline{V} \otimes \overline{V} + n\,\frac{2}{3}\bar{\sigma}\mathbf{I} \right) - \frac{\partial n\,\overline{V}}{\partial \bar{s}} = -\frac{\tau_v}{\tau_p}\, n\,\overline{V} - \bar{D}_x \nabla_\xi n \tag{4.5}$$

$$\frac{\partial}{\partial \tau}\left[n\left(\frac{\overline{V}^2}{2} + \bar{\sigma} \right) \right] + \nabla_\xi \cdot \left(n\left(\frac{\overline{V}^2}{2} + \bar{\sigma} \right) + n\,\frac{2}{3}\bar{\sigma}\,\overline{V} \right) - \frac{\partial}{\partial \bar{s}}\left[n\left(\frac{\overline{V}^2}{2} + \bar{\sigma} \right) \right]$$

$$= -2n\frac{\tau_v}{\tau_p}\left(\frac{\overline{V}^2}{2} + \bar{\sigma}\right) - \bar{D}_x \nabla_\xi \cdot (n\,\overline{V}) + d\,n\,\bar{D}_{\mathbf{V}_d} \tag{4.6}$$

where $\bar{D}_x = D_x/\overline{\mathbf{U}}^2$ and $\bar{D}_{\mathbf{V}_d} = \tau_v D_{\mathbf{V}_d}/\overline{\mathbf{U}}^2$. In the case $\sigma = 0$, $D_x = 0$ and $D_{\mathbf{V}_d} = 0$, we recover the equations used in the laminar case derived in Laurent and Massot (2001). So far the term "multi-fluid" was used for the upwind discretization in the size variable of the semi-fluid model. However, since the semi-fluid model is also composed of a continuous superposition of "fluids" which correspond to the surface conditioned velocity moments, we will indifferently call it semi-fluid or multi-fluid in this paper.

In the case of very small droplets, D_x takes the following asymptotic expression:

$$D_x \approx \frac{2}{d}\,\kappa_p\,\frac{\tau_d}{\tau_p}.$$

The source term in the momentum conservation equation (4.4) then reads

$$-\frac{\tau_v}{\tau_p}\left(n\,\overline{V} + \frac{2}{d}\,\frac{\tau_d\,\kappa_p}{\tau_v\,\overline{\mathbf{U}}^2}\,\nabla_\xi n \right).$$

and can be considered, in the formal singular limit of small s, to be zero. This provides an expression for the mass flux in equation (4.4) which can be rewritten

$$\frac{\partial n}{\partial t} - \nabla_\xi \cdot (\mu\,\nabla_\xi n) - \frac{\partial n}{\partial \bar{s}} = 0, \tag{4.7}$$

with $\mu = 2\tau_d\,\kappa_p/(d\,\tau_v\,\overline{\mathbf{U}}^2)$. Consequently, if we consider the gas turbulence in the white noise limit, i.e. when τ_d approaches zero and turbulence induces a diffusion process in the velocity phase space only (Chandrasekhar (1943), Lightstone and Raithby (1998)), we cannot retrieve the diffusion process in the limit of small particles. Let us also notice that the singular perturbation analysis allows us to relate $\mathbf{V}_d$ and σ to the number density

field n once it is evaluated by solving (4.7). We then not only recover the usual spatial diffusion equation in the limit of small droplets, where the diffusion coefficient is related to a Lagrangian correlation time and a diffusion process coupled to the vaporization one. It is possible to recover as well the relation between the number density field, the associated velocity and the internal energy through the diffusion coefficients $\bar{D}_x$ and $\bar{D}_{\mathbf{V}_d}$.

4.2. *Resolution and results*

It is interesting to notice that the system (4.4-4.6), in the stationary configuration considered, is exactly related to the classical one-dimensional Euler equations where the time has become $1-s$ and where the turbulent dispersion comes into play through source terms involving the defined diffusion coefficients. An initial surface $s_1 = 0.95$ is selected close to the injection point. Initial fields of density, velocity and internal energy as a function of ξ are extracted from the s_1 DNS profiles. The resulting initial value problem for the system of equation is then resolved using a MUSCL second-order extension of a finite-volume method with a minmod slope limiter and explicit second-order time discretization on a fine discretization, which is practicable in this one-dimensional problem.

Comparisons between DNS statistics issued from the Lagrangian dispersion of the droplets and the Eulerian resolution of the multi-fluid model are shown in figures 8 and 9. For both heavy (**T2V1**) and light (**T0V1**) droplets, the evolution of the density of droplets is accurately captured by the multi-fluid formulation (figure 8). Moreover, in the case **T2V1** where the droplets are not strictly following the gas evolution, the Eulerian resolution of the evolution of the droplets' conditioned velocity and internal energy has been captured by the model (figure 9).

5. Conclusions

For the first time, comparisons between a DNS (coupled with a Lagrangian solver) of a statistically stationary turbulent two-phase flow and an Eulerian model dedicated to spray dispersion have been carried out. DNS showed its ability to capture the evolution of some complex interactions between the flow and the vaporizing droplets. Then, the Eulerian multi-fluid model has been resolved and compared with the DNS results. The multi-fluid model proved able to capture the evolution of a polydisperse vaporizing spray in a turbulent environment. This is a very encouraging result for the modeling of complex configurations such as combustion chambers. Indeed, even if more tests and development are needed, the multi-fluid formulation may be an alternative to the actual Lagrangian model, which may have difficulties in representing some phenomena such as coalescence or breakup of the droplets.

Acknowledgments

The authors wish to thank the members of the CTR Summer Program. In particular, the help of their CTR hosts Dr. S. Apte and Dr. H. Pitsch is gratefully acknowledged.

REFERENCES

Batchelor G. K. 1949 Diffusion in a field of homogeneous turbulence. I. Eulerian analysis. *Australian J. Sci. Research. Ser. A*.**2**, 437–450.

Chandrasekhar S. 1943 Stochastic problems in physics and astronomy. *Rev. Mod. Phys.* **15**, (1).

Chanteperdrix G., Villedieu P. and Vila J.P. 2002 A compressible model for separated two-phase flows computations *ASME/ FEDSM'02 Paper* 31141.

Clouet J. F.and Domelevo K. 1997 Solution of a kinetic stochastic equation modeling a spray in a turbulent gas flow. *Math. Models Methods Appl. Sci.* **7**, 239–263.

Domelevo K. & Sainsaulieu L. 1997 A numerical method for the computation of the dispersion of a cloud of particles by a turbulent gas flow field. *J. Comput. Phys.* **133**, 256–278.

Dukowicz, J.K. 1980 A particle-fluid numerical model for liquid sprays. *J. Comput. Phys.* **35**, 229–253.

Kaufmann A., Poinsot T., and Simonin O. 2002 Les of turbulent two-phase flows using an eulerian-eulerian approach. In *Proceedings of the Summer Program 2002*, Center for Turbulence Research, NASA Ames/Stanford Univ.

Laurent L. and Massot M. 2001 Multi-fluid modeling of laminar poly-dispersed spray flames, origin, assumptions and comparison of the sectional and sampling methods. *Combust. Theory and Modelling* **5**, 537–572.

Laurent F., Massot M., and Villedieu P. 2001 Eulerian multi-fluid modeling for the numerical simulation of polydisperse dense liquid spray. Preprint, MAPLY, UMR 5585 Lyon. (http, //maply.univ-lyon1.fr/publis/publiv/2001/335/publi.ps.gz). g

Laurent F., Santoro V., Noskov N., Gomez A., Smooke M.D., and Massot M. 2002 Accurate treatment of size distribution effects in polydispersed spray diffusion flames, multi-fluid modeling, computations and experiments. Preprint, MAPLY, UMR 5585 Lyon. (http, //maply.univ-lyon1.fr/publis/publiv/2002/publis.html).

Lightstone M.F. and Raithby G.D. 1998 A stochastic model of particle dispersion in a turbulent gaseous environment. *Combustion and Flame* **113**, 424–441.

Marchisio D.L., Vigil R.D. & Fox, R.O. 2002 Quadrature method of moments for aggregation-breakage processes. *J. of Colloid and Interface Science*, to appear.

O'Rourke, P.J. 1981 *Collective drop effects on vaporizing liquid sprays. PhD thesis*, University of California/Los Alamos National Laboratory.

Overholt and Pope, S. B. 1998 A deterministic forcing scheme for direct numerical simulation of turbulence. *Computer and Fluid*, **27**,11-28.

Poinsot, T. and Lele, S. K. 1992. Boundary conditions for direct simulations of compressible viscous flows. *J. Comput. Phys.*, **1(101)**,104-129.

Reeks M. W. 1991 On a kinetic equation for the transport of particles in turbulent flows. *Phys. Fluids*, 3, 446–456.

Sainsaulieu L. 1991 *Modélisation, Analyse Mathématique et Numérique d'écoulements diphasiques constitués d'un brouillard de gouttes.* PhD thesis, Ecole Polytechnique.

Taylor G. I. 1921 Diffusion by continuous movements. *Proc. R. Soc. London*, 20, 421–478.

Vallet A., Burluka A.A., and Borghi R. 2001 Development of an Eulerian model for the "atomization" of a liquid jet. *Atomization and Sprays*, 11(5), 521–544.

Vervisch-Guichard, L., Réveillon, J., and Hauguel, R. 2001 Stabilization of a turbulent premixed flame. *Proceedings of the second Symposium on turbulent shear flows phenomena, Stockholm, June 2001.*

Williams F.A. 1958 Spray combustion and atomization. *Phys. Fluids*, 1, 541–545.

Wright, D. L., McGraw, R. & Rosner D. E. 2001 Bivariate extension of the quadrature method of moments for modeling simultaneous coagulation and sintering of particle populations. *J. of Colloid and Interface Sci.*, 236, 242–251.